

Tungsten Carbonitride Films | Very Important Paper |

VIP Synthesis and Characterization of Tungsten Nitrido Amido Guanidinato Complexes as Precursors for Chemical Vapor Deposition of WN_xC_y Thin FilmsMichelle M. Nolan,^{[a][‡]} Alexander J. Touchton,^{[a][‡]} Nathaniel E. Richey,^[a] Ion Ghiviriga,^[a] James R. Rocca,^[b] Khalil A. Abboud,^[a] and Lisa McElwee-White*^[a]

Abstract: Tungsten nitrido amido guanidinato complexes of the type $WN(NR_2)[(NR')_2C(NR_2)]_2$ ($R = Me, Et$; $R' = iPr, Cy$) were synthesized as precursors for aerosol-assisted chemical vapor deposition (AACVD) of WN_xC_y thin films. The reaction of tungsten nitrido amido complexes of the type $WN(NR_2)_3$ ($R = Me, Et$) with two equivalents of a carbodiimide $R'N=C=NR'$ ($R' = iPr, Cy$) resulted in two insertions of a carbodiimide into W–N(amido) bonds, affording bis(guanidinato) amido nitrido

tungsten complexes. These compounds were characterized by ^{14}N NMR, indicating distinctive chemical shifts for each type of N-bound ligand. Crystallographic structure determination of $WN(NMe_2)[(NiPr)_2C(NMe_2)]_2$ showed the guanidinato ligands to be non-equivalent. The complex $WN(NMe_2)[(NiPr)_2C(NMe_2)]_2$ was demonstrated to serve as a precursor for AACVD of WN_xC_y thin films, resulting in featureless, X-ray amorphous thin films for growth temperatures 200–400 °C.

Introduction

Chemical vapor deposition (CVD) is a critical tool in the electronics industry for the fabrication of thin film and nanostructure materials. During CVD, vapor-phase precursors undergo a chemical reaction to deposit a material of interest on a heated substrate. Some of the key advantages of CVD over other physical deposition methods include its high deposition rates, control over film thicknesses and morphologies, efficacy in conformal film growth, and flexibility towards process modifications for specific applications.^[1] Additional control over deposit stoichiometry and the prevention of premature precursor reaction are accessible through the use of single source precursors, in which all components of the deposited material derive from a single complex.^[2] The design of single source precursors for CVD represents a significant challenge because it relies on optimizing many compound properties, including volatility, toxicity, stability, and decomposition reproducibility.^[2b]

We have used aerosol-assisted (AA)CVD of tungsten carbonitride (WN_xC_y) as a platform for exploring the mechanism-based design of single source CVD precursors.^[3] This material had been considered as a candidate for copper diffusion barriers in integrated circuits due to its low electrical resistivity, high

thermal stability, and minimal chemical reactivity with existing circuit materials.^[4] Previously reported single source precursors for deposition of WN_xC_y have utilized N-bound ligands such as nitrido, imido, hydrazido, amido, guanidinato, and amidinato moieties to provide the nitrogen in the resulting material.^[5] Optimization of the precursors has primarily targeted low temperature deposition (<350 °C) to minimize the thermal damage to the substrate. Our studies of tungsten nitrido complexes of the type $WN(NR_2)_3$ demonstrated that the $W\equiv N$ and $W-NR_2$ moieties are acceptable sources of N in depositions carried out at temperatures as low as 125 °C. In addition, variation of the substituents in the amido moieties of $WN(NR_2)_3$ provided a means to tune the precursor volatility.^[5g,6]

A general strategy to improve the thermal stability of a CVD precursor while maintaining volatility is the addition of chelating ligands, such as guanidinato ligands.^[7] Guanidinato ligands are N-bound, bidentate ligands which have been extensively employed in CVD precursors due to their electronic versatility, thermal stability, and nitrogen contribution to deposits.^[8] Late transition-metal guanidates have been used in deposition of metal films, including Cu and Ni.^[7,9] However, early transition-metal guanidinate precursors have yielded metal nitride and metal carbonitride thin films under CVD conditions. Mixed guanidinato amido complexes of Ta and Nb have been employed in the CVD of TaN and NbN thin films.^[10] Growth of ZrN_xC_y and TiN_xC_y films was achieved from bis(guanidinato) complexes.^[8,11]

Our previous study of the tungsten imido guanidinato precursor $W(NiPr)Cl_3[(iPrN)_2CNMe_2]$ demonstrated that guanidinato ligands are suitable for use in precursors for the AACVD of WN_xC_y .^[5d] We now report the synthesis of tungsten nitrido am-

[a] Department of Chemistry, University of Florida
Gainesville, FL 32611-27200, USA
E-mail: lmwhite@chem.ufl.edu
<http://lmwhite.chem.ufl.edu/>

[b] McKnight Brain Institute, University of Florida
Gainesville, FL 32610-0015, USA

[‡] M. M. N. and A. J. T. made equal contributions to the work.

Supporting information and ORCID(s) from the author(s) for this article are available on the WWW under <https://doi.org/10.1002/ejic.201701225>.

ligands *cis* to one another, as shown in Figure 1. Selected bond lengths and angles are reported in Table 2. The nitrido W≡N bond length [W1–N1, 1.6906(12) Å] is similar to the 1.680(2) Å previously observed for **2**.^[5f] The amido W–N bond length of **1** [W1–N5, 1.9552(1) Å] is also similar to the parent compound **2**, which had an average W–N bond length of 1.952(2) Å for its three amido ligands. The sum of the bond angles around the amido nitrogen is 359.99°, indicating sp² hybridization of the amido N.

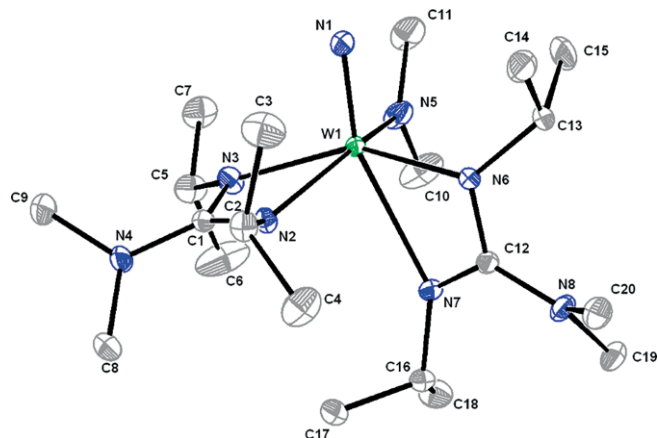


Figure 1. Displacement ellipsoid model of **1**; ellipsoids are shown at 50% probability. Protons are omitted for clarity.

Table 2. Selected bond lengths [Å] and angles [°] for **1**.

W1–N1	1.6906(12)	N1–W1–N5	96.57(6)
W1–N5	1.9552(12)	N1–W1–N6	98.18(5)
W1–N6	2.0637(11)	N1–W1–N3	103.60(5)
W1–N3	2.1749(11)	N6–W1–N3	149.28(4)
W1–N2	2.1892(11)	N1–W1–N2	100.66(5)
W1–N7	2.5698(11)	N5–W1–N2	153.79(5)
N2–C1	1.3307(16)	N3–W1–N2	60.29(4)
N3–C1	1.3354(17)	N1–W1–N7	154.94(5)
N4–C1	1.3854(17)	N6–W1–N7	56.77(4)
N6–C12	1.3808(17)	N2–C1–N3	110.58(11)
N7–C12	1.3063(17)	N7–C12–N6	113.49(11)
N8–C12	1.3876(16)		

The two guanidinato ligands are non-equivalent, with their W–N bond lengths and ligand bite angles varying based on their positions relative to the strongly π-donating nitrido moiety. The guanidinato ligand bound by N2 and N3 exhibits two similar W–N bond lengths [W1–N2, 2.1892(11) Å and W1–N3, 2.1749(11) Å]. However, the guanidinato ligand bound by N6 and N7 shows two significantly different bond lengths [W1–N6, 2.0637(11) Å and W1–N7, 2.5698(11) Å]. The *trans* influence imparted by the nitrido ligand is observed in the lengthening of the W1–N7 bond, similar to reported W^{VI}, Ta^V and Nb^V imido complexes.^[5c,10b] The greater degree of bond alternation of the C–N bonds [N6–C12 1.3808(17) and N7–C12 1.3063(17) Å] and the long W1–N7 distance in the unsymmetrical guanidinato ligand are consistent with a substantial contribution from the resonance structure shown in Figure 2.

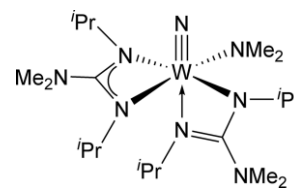


Figure 2. Major resonance structure for **1**.

NMR Characterization of **1** and **3**

Because of the large numbers of similar chemical shifts in complex **1**, ¹H–¹³C indirect detection experiments were performed in [D₈]toluene at –50 °C to assign the signals. The spectra were consistent with two guanidinato and one dimethylamido moieties, with 14 non-equivalent methyl groups (Figure S-9, Supporting Information) in agreement with the structure determined by X-ray diffractometry. Attempts to obtain the ¹⁵N chemical shifts of **1** by ¹H–¹⁵N indirect detection experiments at –25 °C were thwarted by the low solubility of **1**. At 25 °C, the solubility was better, but line broadening of the ¹H NMR signals for the guanidinato –NMe₂ groups resulted in the exocyclic nitrogen in the guanidinato groups not being detected. Detected ¹H, ¹³C, and ¹⁵N chemical shifts for **1** are given in Figure 3.

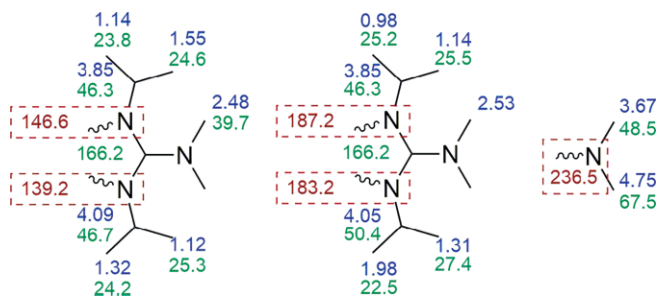


Figure 3. ¹H (blue), ¹³C (green), and ¹⁵N (red) chemical shifts (ppm) of **1** as measured by ¹H–¹³C and ¹H–¹⁵N indirect detection in [D₈]toluene at 25 °C. Unlabeled N atoms were not detected.

The ¹H–¹³C gHMBC spectrum of compound **3** in [D₈]toluene at –50 °C facilitated assignment of the methine and methyl resonances in two guanidinato and one dimethylamido moieties (Figure 4), in agreement with a structure similar of that of com-

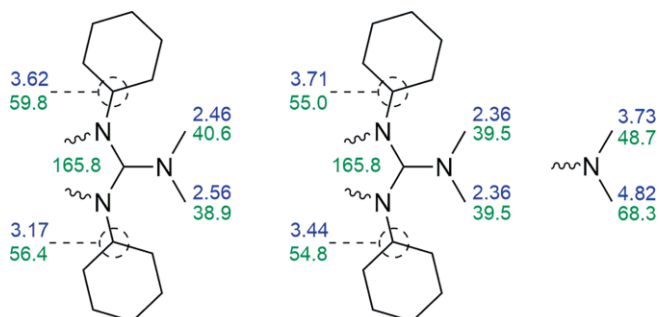


Figure 4. Selected ¹H (blue) and ¹³C (green) chemical shifts (ppm) of **3** as measured by ¹H–¹³C indirect detection in [D₈]toluene at –50 °C.

pound **1**. All 20 methylene groups were evident in the gHSQC spectrum but extensive overlap made the assignment of individual chemical shifts impossible. The solubility of **3** was insufficient for indirect detection of ^{15}N .

When ^1H - ^{15}N indirect detection experiments failed to afford a signal for the nitrido moiety due to insufficient long range coupling, the ^{14}N NMR spectrum of **1** was obtained (Figure 5). In the ^{14}N NMR spectrum of **1**, resonances for the metal bound N-atoms can be clearly resolved despite the large linewidths associated with the quadrupolar ^{14}N nucleus.^[13] The chemical shifts observed for the guanidinato and amido moieties of **1** correlate with the resonances observed by ^1H - ^{15}N indirect detection. The terminal nitrido resonance in **1** can be assigned as the broad peak at $\delta = 753$ ppm, with the analogous signal of **2** appearing at $\delta = 760$ ppm. Both of these values are consistent with other previously reported chemical shifts for the nitrido moiety in group VI metal complexes.^[14]

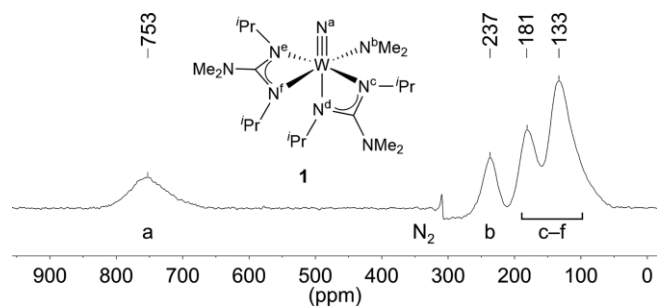
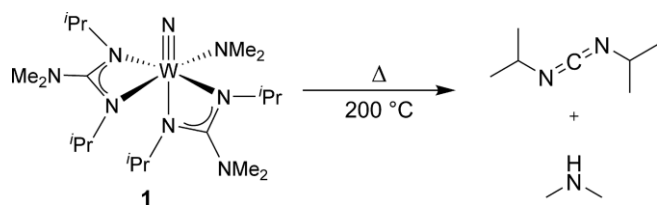


Figure 5. ^{14}N NMR spectrum of **1** in $[\text{D}_6]\text{benzene}$ at 25°C .

Thermolysis of **1**

Because CVD is a thermal process, examining the pyrolysis of a precursor under non-deposition conditions can provide valuable insight into possible breakdown pathways that occur during deposition. The thermal decomposition of **1** was investigated by pyrolysis of neat samples and by thermogravimetric analysis (TGA). Decomposition products from solid state pyrolysis were isolated by heating a neat sample of **1** to 200°C under 1 atm of N_2 and condensing the volatile components at 77 K. Analysis of the condensate by ^1H NMR, ^{13}C NMR, FTIR, and GC-MS revealed the presence of dimethylamine and diisopropylcarbodiimide **7** (Scheme 2). Isolation of DIC indicates that the deinsertion of carbodiimide is an accessible decomposition pathway. This deinsertion would regenerate the original dimethylamido ligand, which could then decompose further through pathways previously established for **2**. For example, the presence of dimethylamine is consistent with the thermolysis



Scheme 2. Thermolysis of **1**.

of **2** under similar conditions.^[6] Analogous deinsertion has been reported for other guanidinato complexes.^[7,9c,15] The TGA of **1** (Figure S-10) indicates an initial decomposition step at 200°C . The residual mass of 63 % corresponds to the loss of one guanidinato ligand and one amido ligand, consistent with the products observed by GC-El-MS.

Film Growth and Characterization

Compound **1** was tested as a single source precursor for the AACVD of WN_xC_y . The AACVD was performed from heptane solutions of **1** at substrate temperatures between 200 – 400°C , resulting in dark, iridescent deposited films. Films exhibited good adhesion to the Si substrates and passed a qualitative peel test using adhesive tape. Deposited material at all growth temperatures was found to be amorphous by XRD. The morphologies of the deposits were determined by SEM, as shown in Figure 6. At temperatures of 200 and 300°C , films resembled Stranski–Krastanov type growth: a layer of material covered the substrate surfaces with islands of growth appearing on top. At 400°C , these islands appeared to grow into more pronounced vertical features. Cross-sectional SEM indicated average film thicknesses of 29, 25, and $14\ \mu\text{m}$ at deposition temperatures of 200 , 300 , and 400°C , respectively.

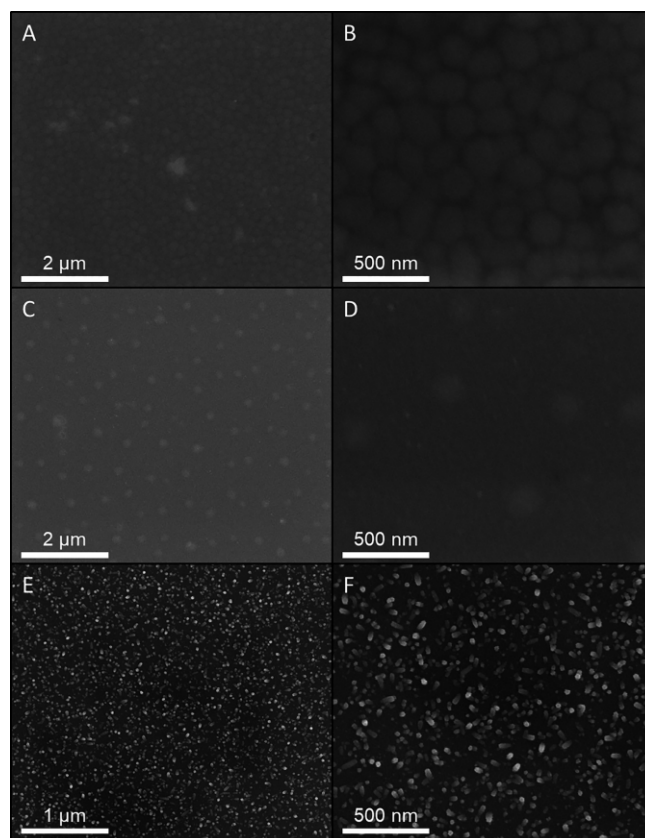


Figure 6. SEM images of WN_xC_y films deposited at (a,b) 200°C , (c,d) 300°C , and (e, f) 400°C .

The compositions of the deposits were determined by XPS. Nitrogen content ranged from 11.6 to 17.0 atom percent of the

deposits, whereas tungsten comprised approximately 20 at. %. Carbon accounted for approximately 20 to 30 at. % of the deposited material. These deposits showed higher N and C content, but lower W content, than the deposits previously grown from $WN(NR_2)_3$ complexes.^[5g,5h,6] Oxygen was present in significant amounts in all films and was attributed to post-deposition oxidation of the samples when handling in air prior to obtaining XPS. Due to the amorphous nature of the films, significant in-diffusion of oxygen is possible post-growth. Although depth profiling was not carried out for these samples, we have previously determined by AES depth profiling that oxygen content in our WN_xC_y films is highest in the upper layers, consistent with oxidation during handling.^[5b]

High-resolution XPS was taken to determine the chemical environment of the different elements by comparison to known data.^[16] Deconvolution of the W 4f signal revealed two signals for deposits grown at 400 °C, and three peaks at 200 and 300 °C (Figure 7a). For all deposits, a W 4f_{7/2} peak was observed with a binding energy (BE) of 33.2 eV with the corresponding W 4f_{5/2} peak at a BE of 35.3 eV. Peaks were also observed in all deposits with BEs of 35.4 eV, representing W 4f_{7/2}, and 37.6 eV for 4f_{5/2}. For deposits grown at 300 °C and below, W 4f_{7/2} and 4f_{5/2} peaks were observed with BEs of 34.2 and 36.4 eV, respectively. The W 4f_{7/2} peaks at BEs of 33.2, 34.2, and 35.4 eV are consistent with values reported for W in the +4, +5, and +6 oxidation states, respectively.^[16] The W 4f_{7/2} peaks at 35.4 and 33.2 eV have previously been observed from deposits grown

from $WN(NR_2)_3$ complexes. However, no deposit from **1** showed a peak at 31.5 eV which has previously been reported for W metal observed in depositions from $WN(NR_2)_3$.^[5h] It is possible that any W metal formed in these samples was oxidized during handling.

Deconvolution of the N 1s signal revealed two peaks at all temperatures (Figure 7b). A peak with a BE of 400.0 eV was observed at all temperatures and has been assigned as CN_x , which typically exhibits BEs of 398.5 to 400.6 eV. A second peak was observed at BE 397.4 eV, corresponding to WN. This peak comprised most of the N at deposits grown at 400 °C and was attributed to more extensive decomposition of the precursor than was seen in deposits from lower temperature growths.

Likewise, the C 1s signal was deconvoluted into two distinct signals (Figure 7c). Amorphous C is typically observed at a BE of 284.6 eV and can be observed at all growth temperatures. This peak was more intense in deposits grown at 400 °C, which is consistent with increased solvent decomposition during higher temperature growth. A peak at BE 286.2 eV was also observed at all growth temperatures and was attributed to CN_x in the deposits. Interestingly, no peaks were observed for carbidic C, which has a characteristic BE of 283.5 eV. Oxide was observed in samples from all growth temperatures due to the rapid oxidation of WN_xC_y deposits when handling the samples in air prior to analysis. This oxygen peak was assigned as WO_3 with a BE of 530.7 eV and used as the internal reference for samples after sputtering (Figure 7d).

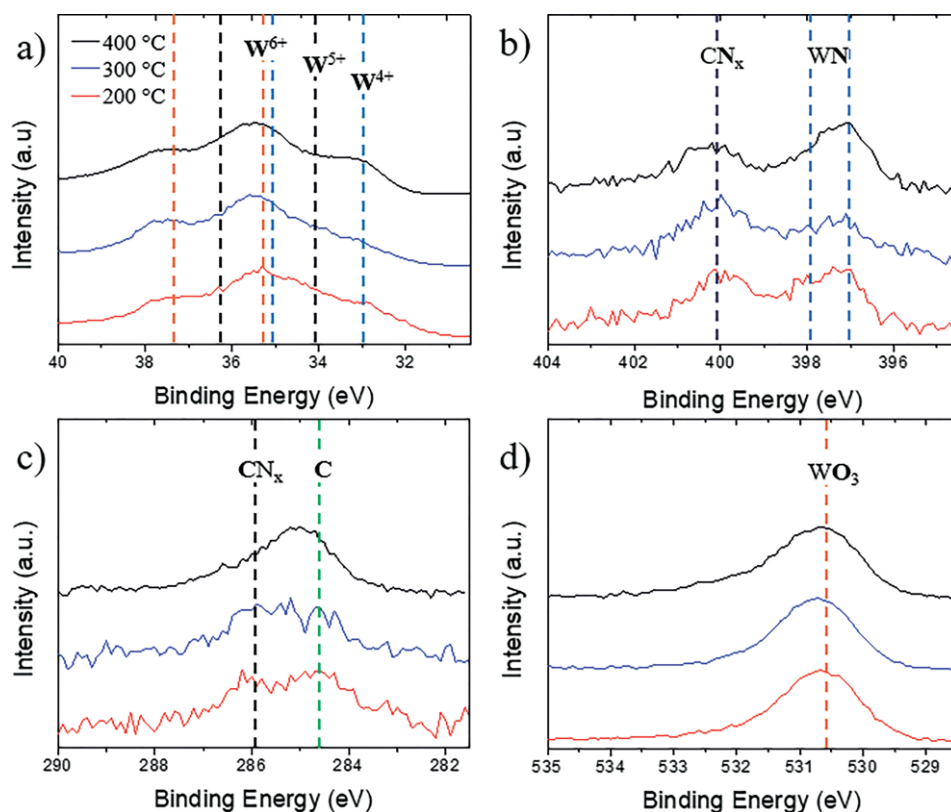


Figure 7. XPS spectra for primary peaks of (a) W 4f_{7/2} and 4f_{5/2}, (b) N 1s, (c) C 1s, and (d) O 1s. Dashed lines are included for visual reference.

Conclusions

In conclusion, several tungsten nitrido amido guanidinato complexes of the type $WN(NR_2)[(NR')_2C(NR_2)]_2$ have been prepared and characterized. The thermal decomposition of $WN(NMe_2)[(iPrN)_2C(NMe_2)]_2$ (**1**) was studied and was found to be consistent with its performance as a viable precursor for the deposition of WN_xC_y thin films.

Experimental Section

General Procedures: All manipulations were performed under an inert atmosphere of dry N_2 using standard Schlenk and glovebox techniques. $[D_6]$ benzene and $[D_8]$ toluene were purchased from Cambridge Isotope Laboratories, Inc., degassed, and stored over activated 3 Å molecular sieves (15 %, w/v) for at least 24 h prior to use. Heptane was dried and deoxygenated using an MBraun MB-SPS solvent purification system and stored over activated 3 Å molecular sieves. Anhydrous pentane and N,N' -dicyclohexylcarbodiimide (DCC) were purchased from Sigma Aldrich and used as received. The N,N' -diisopropylcarbodiimide (DIC) was purchased from Sigma-Aldrich, degassed, and stored over activated 3 Å molecular sieves (15 %, w/v) prior to use. Compound **4** was synthesized as described previously.^[6] 1H and ^{13}C NMR spectra were recorded using Mercury 300 MHz spectrometers utilizing residual protons of the deuterated solvents as reference peaks. Indirect detection spectra for compounds **1** and **3** were run on a 3-RF channel 500 MHz Varian Inova spectrometer equipped with a 5 mm indirect detection probe with z-axis gradients. The chemical shifts were referenced to tetramethylsilane for 1H (all coupling values are 7 Hz, unless otherwise specified) and ^{13}C , and to liquid ammonia for ^{15}N , using the Ξ values from the IUPAC recommendations.^[17] Some ^{13}C and all ^{14}N NMR spectra were acquired using a Bruker Avance III 600 MHz spectrometer, using dissolved N_2 as the reference; a more detailed experimental procedure is included in the Supporting Information. Mass spectra of synthesized compounds were obtained with an Agilent 6200 ESI-TOF mass spectrometer using the direct analysis in real time time-of-flight (DART-TOF) mode of operation. Samples for thermogravimetric analysis were prepared and sealed in crimped 40 μ L aluminum sample pans inside an Ar atmosphere glovebox. Thermogravimetric analyses were performed using a Mettler TGA/sDTA 851e: the pans were pierced using a Mettler piercing kit and heated at 10 °C/min from room temperature to 600 °C under an N_2 atmosphere. Mass spectra of the condensed pyrolysis products were obtained by GC/EL-MS using a ThermoScientific DSQ II mass spectrometer and a ThermoScientific Trace GC Ultra gas chromatograph equipped with a Restek Corp. tabilwax-DA column. Elemental analysis results were obtained from Robertson Microlit. Powder XRD patterns of the deposited films were collected using a PANalytical X'Pert³ Powder diffractometer. The surface morphologies of deposited films were imaged using an FEI Nova NanoSEM 430 microscope. The elemental compositions of deposited films were determined by XPS using an ULVAC-PHI XPS, and spectra were deconvoluted using the MultiPak software. Pretreatment of the films for XPS involved sputtering for 2 min to remove surface contamination.

$WN(NMe_2)_3$ (2**):** Compound **2** was synthesized as previously reported and characterized by comparison to literature data.^[5f] ^{14}N NMR (C_6D_6 , 43 MHz): $\delta = 159$ ($W-NMe_2$), 760 ($W=N$).

$WN(NMe_2)[(iPrN)_2C(NMe_2)]_2$ (1**):** Inside the glovebox, **2** (2.4 g, 7.3 mmol) was combined with 200 mL of pentane in a 250 mL Schlenk flask to form a light tan suspension. To this suspension, DIC (2.4 mL, 15 mmol) was added in a single aliquot. The reaction mixture

quickly darkened to an amber color. This mixture was allowed to stir for 10 min and then was filtered through a fine frit to yield a yellow filtrate, which was concentrated under vacuum. The mother liquor was removed and the pure product was dried under vacuum, yielding 2.9 g (5.0 mmol, 69 %) of **1** as yellow crystals. 1H NMR (500 MHz, C_6D_6): $\delta = 1.03$ [d, 3 H, $CH(CH_3)_2$], 1.16 [d, 3 H, $CH(CH_3)_2$], 1.18 [d, 3 H, $CH(CH_3)_2$], 1.18 [d, 3 H, $CH(CH_3)_2$], 1.37 [d, 3 H, $CH(CH_3)_2$], 1.39 [d, 3 H, $CH(CH_3)_2$], 1.63 [d, 3 H, $CH(CH_3)_2$], 2.07 [d, 3 H, $CH(CH_3)_2$], 2.48 [s, 6 H, $CN(CH_3)_2$], 2.53 [s, 6 H, $CN(CH_3)_2$], 3.60 [sept, 1 H, $CH(CH_3)_2$], 3.71 [s, 3 H, $WN(CH_3)CH_3$], 3.89 [sept, 1 H, $CH(CH_3)_2$], 4.10 [sept, 1 H, $CH(CH_3)_2$], 4.12 [sept, 1 H, $CH(CH_3)_2$], 4.82 [s, 3 H, $WN(CH_3)CH_3$] ppm. ^{13}C NMR (C_6D_6 , 151 MHz): 22.9, 24.1, 24.6, 25.1, 25.6, 25.7, 25.9, 27.8 [$CH(CH_3)_2$], 40.1 [$CN(CH_3)_2$], 46.6 [$CH(CH_3)_2$], 47.1 [$CH(CH_3)_2$], 47.5 [$CH(CH_3)_2$], 48.9 [$WN(CH_3)CH_3$], 50.8 [$CH(CH_3)_2$], 68.0 [$WN(CH_3)CH_3$], 166.2, 166.7 (N_3C). ^{15}N NMR ($C_6D_5CD_3$, 51 MHz): $\delta = 139.2$, 146.6, 183.2, 187.2 { $W[(iPrN)_2C(NMe_2)]_2$ }, 236.5 ($WNMe_2$). ^{14}N NMR (C_6D_6 , 43 MHz): $\delta = 133$, 181 { $W[(iPrN)_2C(NMe_2)]_2$ }, 237 ($WNMe_2$), 753 ($W=N$) ppm. MS (DART-TOF): calcd. for $[M + H]^+$ 583.3428, found 583.3440. $C_{20}H_{46}N_8W$ (582.49): calcd. C 41.24, H 7.96, N 19.24; found C 40.83, H 7.80, N 18.87.

$WN(NMe_2)[(CyN)_2C(NMe_2)]_2$ (3**):** Inside the glovebox, **2** (0.26 g, 0.77 mmol) was combined with 15 mL of pentane in a glass vial to form a tan suspension. After agitating the mixture, DCC (0.43 g, 2.1 mmol) was added, and a color change to from tan to yellow was observed. The reaction mixture was allowed to sit for 5 min and then was filtered through a fine frit to yield a yellow filtrate, which was transferred to a clean vial. The solution was concentrated under vacuum and left in the glovebox freezer (-15 °C) overnight. The mother liquor was removed and the pure product was dried under vacuum to yield 0.23 g (0.32 mmol, 41 %) of **3** as yellow crystals. 1H NMR (C_6D_6 , 500 MHz): $\delta = 1.02$ – 2.17 [m, 37 H, $CH(CH_2)_5$], 2.30 [m, 1 H, $CH(CH_2)_5$], 2.43 [m, 1 H, $CH(CH_2)_5$], 2.54 [s, 6 H, $CN(CH_3)_2$], 2.61 [s, 6 H, $CN(CH_3)_2$], 3.26 [m, 1 H, $CH(CH_2)_5$], 3.42 [m, 1 H, $CH(CH_2)_5$], 3.21 [m, 1 H, $CH(CH_2)_5$], 3.53 [m, 1 H, $CH(CH_2)_5$], 3.70 [m, 1 H, $CH(CH_2)_5$], 3.77 [s, 3 H, $WN(CH_3)CH_3$], 4.87 [s, 3 H, $WN(CH_3)CH_3$] ppm. ^{13}C NMR (C_6D_6 , 151 MHz): $\delta = 26.20$, 26.31, 26.46, 26.54, 26.63, 26.66, 26.68, 26.92, 27.03, 27.43, 27.53, 33.34, 34.03, 35.30, 35.40, 35.44, 35.84, 36.48, 36.65, 38.79 [$NCH(CH_2)_5$], 40.24 [$N_2CN(CH_3)_2$], 48.92 [$WN(CH_3)CH_3$], 55.50, 55.90, 56.85, 60.16 [$NCH(CH_2)_5$], 68.17 [$WN(CH_3)CH_3$], 166.28, 166.54 (N_3C) ppm. MS (DART-TOF): calcd. for $[M + H]^+$ 743.4680, found 743.4695.

$WN(Net_2)[(iPrN)_2C(Net_2)]_2$ (5**):** Inside the glovebox, **4** (0.28 g, 0.70 mmol) was combined with 15 mL of pentane in a glass vial to form an amber solution. After briefly agitating the mixture, DIC (0.22 mL, 1.40 mmol) was added. No color change was observed. The reaction mixture was allowed to sit for 5 min and then was filtered through a fine frit to yield an amber filtrate, which was transferred to a clean vial. The solution was concentrated under vacuum and left in the glovebox freezer (-15 °C) overnight. The mother liquor was removed and the pure product was dried under vacuum, providing 0.1609 g (0.24 mmol, 35 %) of **5** as amber crystals. 1H NMR (C_6D_6 , 500 MHz): $\delta = 0.91$ (t, 6 H, CH_2CH_3), 0.98 (t, 3 H, CH_2CH_3), 1.03 [d, 3 H, $CH(CH_3)_2$], 1.16 [d, 3 H, $CH(CH_3)_2$], 1.17 [d, 3 H, $CH(CH_3)_2$], 1.24 [d, 3 H, $CH(CH_3)_2$], 1.42 [d, 3 H, $CH(CH_3)_2$], 1.50 (t, 3 H, CH_2CH_3), 1.51 [d, 3 H, $CH(CH_3)_2$], 1.68 [d, 3 H, $CH(CH_3)_2$], 2.06 [d, 3 H, $CH(CH_3)_2$], 2.84, 2.86, 2.91, 3.05 [q, 8 H, $CN(CH_2CH_3)_2$], 3.54 [q, 1 H, $WNC(H)HCH_3$], 3.60 [sept, 1 H, $CH(CH_3)_2$], 3.85 [sept, 1 H, $CH(CH_3)_2$], 4.14 [sept, 1 H, $CH(CH_3)_2$], 4.16 [sept, 1 H, $CH(CH_3)_2$], 4.88 [q, 1 H, $WNC(H)HCH_3$], 4.96 [q, 1 H, $WNC(H)HCH_3$], 5.61 [q, 1 H, $WNC(H)HCH_3$] ppm. ^{13}C NMR (C_6D_6 , 75 MHz): $\delta = 13.8$, 14.1, 14.2, 15.8, 16.9 (CH_2CH_3), 23.2, 23.8, 24.8, 24.9, 25.2, 25.6, 25.7, 29.0 [$CH(CH_3)_2$], 41.6, 43.27, 43.5 [$CN(CH_2CH_3)_2$], 46.9 [$CH(CH_3)_2$], 47.0

[CH(CH₃)₂], 48.1 [CH(CH₃)₂], 49.7 (WNCH₂CH₃), 50.2 [CH(CH₃)₂], 67.3 (WNCH₂CH₃), 166.9, 167.6 (N₃C) ppm. MS (DART-TOF): calcd. for [M + H]⁺ 667.4367, found 667.4342.

WN(NEt₂)[(CyN)₂C(NEt₂)]₂ (6): Inside the glovebox, **4** (0.22 g, 0.53 mmol) was combined with 15 mL of pentane in a glass vial to form an amber solution. After briefly agitating the mixture, DCC (0.33 g, 1.6 mmol) was added. The color of the solution lightened slightly after addition. The reaction mixture was allowed to sit for 5 min and then was filtered through a fine frit. The resulting amber filtrate was transferred to a clean glass vial. The solution was concentrated under vacuum and left in the glovebox freezer (-15 °C) overnight. The mother liquor was removed and the pure product was dried under vacuum, providing 0.25 g (0.30 mmol, 56 %) of **6** as yellow crystals. ¹H NMR (C₆D₆, 500 MHz): δ = 0.87 (t, 3 H, CH₂CH₃), 0.97 (t, 9 H, CH₂CH₃), 1.04 (t, 3 H, CH₂CH₃), 1.52–1.20 [m, 17 H, NCH(CH₂)₅], 1.55 (t, 3 H, CH₂CH₃), 2.15–1.58 [m, 19 H, NCH(CH₂)₅], 2.33 [m, 1 H, NCH(CH₂)₅], 2.47 [m, 1 H, NCH(CH₂)₅], 2.73 [m, 1 H, NCH(CH₂)₅], 2.92, 3.00, 3.02, 3.17 [q, 8 H, CN(CH₂CH₃)₂], 3.23 [m, 1 H, NCH(CH₂)₅], 3.45 [m, 1 H, NCH(CH₂)₅], 3.45 [m, 1 H, NCH(CH₂)₅], 3.60 [q, 1 H, WNC(H)HCH₃], 3.74 [m, 2 H, NCH(CH₂)₅], 4.91 [q, 1 H, WNC(H)HCH₃], 5.04 [q, 1 H, WNC(H)HCH₃], 5.66 [q, 1 H, WNC(H)HCH₃] ppm. ¹³C NMR (C₆D₆, 75 MHz): δ = 13.8, 14.1, 14.2, 15.8, 16.9 (CH₂CH₃), 23.2, 23.8, 24.8, 24.9, 25.2, 25.6, 25.7, 29.0 [CH(CH₃)₂], 41.6, 43.27, 43.5 [CN(CH₂CH₃)₂], 46.9 [CH(CH₃)₂], 47.0 [CH(CH₃)₂], 48.1 [CH(CH₃)₂], 49.7 (WNCH₂CH₃), 50.2 [CH(CH₃)₂], 67.3 (WNCH₂CH₃), 166.9, 167.6 (N₃C) ppm. MS (DART-TOF): calcd. for [M + H]⁺ 827.5619, found 827.5591.

Film Growth Studies: Silicon with native silicon dioxide (Si/SiO₂, n-type, <100>) was cut into squares of approximately 1 cm² and cleaned in boiling 2-propanol, acetone, and methanol for 3 min each. The substrates were then placed onto the heating stand, placed under vacuum (200–300 m Torr), and heated to the desired temperature. Precursor **1** was dissolved in 20 mL of heptane at a concentration of 0.051 M and added to a glass trap under inert atmosphere. The trap was then connected to the N₂ inlet of the reactor; N₂ was flowed through the trap for 10 min before connecting to the transfer line. The pressure of the reaction chamber was increased to 350 Torr and the transfer line was heated to 50 °C. The trap was then opened to the reaction chamber and nebulization of the solution was started. During the course of the deposition (typically 60 min), N₂ flow was maintained at 200 sccm and the pressure was maintained at 350 Torr. Once all of the solution had been nebulized, the pressure of the reaction chamber was increased to atmospheric pressure and the substrates were cooled to room temperature.

Crystallographic Structure Determination for 1: X-ray intensity data were collected at 100 K on a Bruker DUO diffractometer using Mo-K_α radiation (λ = 0.71073 Å) and an APEXII CCD area detector. Raw data frames were read by the program SAINT¹⁸ and integrated using 3D profiling algorithms. The resulting data were reduced to produce *hkl* reflections and their intensities and estimated standard deviations. The data were corrected for Lorentz and polarization effects and numerical absorption corrections were applied based on indexed and measured faces. The structure was solved and refined in SHELXL2014,¹⁹ using full-matrix least-squares refinement. The non-H atoms were refined with anisotropic thermal parameters and all of the H atoms were calculated in idealized positions and refined riding on their parent atoms. In the final cycle of refinement, 5986 reflections (of which 5832 are observed with I > 2σ) were used to refine 276 parameters and the resulting R₁, wR₂ and S (goodness of fit) were 1.05 %, 2.47 % and 1.122, respectively. The refinement was carried out by minimizing the wR₂ function using

F² rather than F values. R₁ is calculated to provide a reference to the conventional R value but its function is not minimized.

CCDC 1563665 (for **1**) contains the supplementary crystallographic data for this paper. These data can be obtained free of charge from The Cambridge Crystallographic Data Centre.

Acknowledgments

Financial support of this work was provided by the University of Florida as matching funds for the UF Beckman Scholars Program. A portion of the work was performed in the University of Florida's McKnight Brain Institute at the National High Magnetic Field Laboratory's AMRIS Facility, which is supported by National Science Foundation Cooperative Agreement No. DMR-1157490 and the State of Florida. The magnetic resonance instrumentation was supported in part by an NIH award, S10RR031637. We thank Prof. Aaron Odom for helpful discussion on ¹⁴N NMR spectroscopy. K. A. A. wishes to acknowledge the National Science Foundation and the University of Florida for funding of the purchase of the X-ray equipment. The Major Analytical Instrumentation Center of the Engineering Department at the University of Florida for provided the materials characterization equipment. Thermogravimetric analysis of **1** was performed by Roman Korotkov (Arkema, Inc.).

Keywords: Chemical vapor deposition · Inorganic synthesis · Precursor design · Thin films · Tungsten

- [1] a) H. O. Pierson, *Handbook of Chemical Vapor Deposition (CVD)*, Vol. 2, Noyes Publications, Park Ridge, NJ, **1999**; b) P. Marchand, I. A. Hassan, I. P. Parkin, C. J. Carmalt, *Dalton Trans.* **2013**, 42, 9406–9422.
- [2] a) A. Kafizas, C. J. Carmalt, I. P. Parkin, *Coord. Chem. Rev.* **2013**, 257, 2073–2119; b) P. Marchand, C. J. Carmalt, *Coord. Chem. Rev.* **2013**, 257, 3202–3221.
- [3] a) L. McElwee-White, *Dalton Trans.* **2006**, 5327–5333; b) L. McElwee-White, J. Koller, D. Kim, T. J. Anderson, *ECS Trans.* **2009**, 25, 161–171.
- [4] B. H. Lee, K. Yong, *J. Vac. Sci. Technol. B: Microelectron. Nanometer Struct.-Process. Meas. Phenom.* **2004**, 22, 2375–2379.
- [5] a) O. J. Bchir, K. M. Green, M. S. Hlad, T. J. Anderson, B. C. Brooks, C. B. Wilder, D. H. Powell, L. McElwee-White, *J. Organomet. Chem.* **2003**, 684, 338–350; b) O. J. Bchir, S. W. Johnston, A. C. Cuadra, T. J. Anderson, C. G. Ortiz, B. C. Brooks, D. H. Powell, L. McElwee-White, *J. Cryst. Growth* **2003**, 249, 262–274; c) C. B. Wilder, L. L. Reitfort, K. A. Abboud, L. McElwee-White, *Inorg. Chem.* **2006**, 45, 263–268; d) H. M. Ajmera, A. T. Heitsch, T. J. Anderson, C. B. Wilder, L. L. Reitfort, L. McElwee-White, D. P. Norton, *J. Vac. Sci. Technol. B* **2008**, 26, 1800–1807; e) H. M. Ajmera, T. J. Anderson, J. Koller, L. McElwee-White, D. P. Norton, *Thin Solid Films* **2009**, 517, 6038–6045; f) K. R. McClain, C. O'Donohue, Z. Shi, A. V. Walker, K. A. Abboud, T. Anderson, L. McElwee-White, *Eur. J. Inorg. Chem.* **2012**, 4579–4584; g) A. Koley, C. T. O'Donohue, M. M. Nolan, K. R. McClain, R. O. Bonsu, R. Y. Korotkov, T. Anderson, L. McElwee-White, *Chem. Mater.* **2015**, 27, 8326–8336; h) C. T. O'Donohue, K. R. McClain, A. Koley, J. C. Revelli, L. McElwee-White, T. J. Anderson, *ECS J. Solid State Sci. Technol.* **2014**, 4, N3180–N3187.
- [6] K. R. McClain, C. O'Donohue, A. Koley, R. O. Bonsu, K. A. Abboud, J. C. Revelli, T. J. Anderson, L. McElwee-White, *J. Am. Chem. Soc.* **2014**, 136, 1650–1662.
- [7] J. P. Coyle, W. H. Monillas, G. P. A. Yap, S. T. Barry, *Inorg. Chem.* **2008**, 47, 683–689.
- [8] S. E. Potts, C. J. Carmalt, C. S. Blackman, F. Abou-Chahine, D. Pugh, H. O. Davies, *Organometallics* **2009**, 28, 1838–1844.
- [9] a) Z. Li, A. Rahtu, R. G. Gordon, *J. Electrochem. Soc.* **2006**, 153, C787–C794; b) Z. Li, R. G. Gordon, V. Pallem, H. Li, D. V. Shenai, *Chem. Mater.*

- 2010**, 22, 3060–3066; c) S. T. Barry, *Coord. Chem. Rev.* **2013**, 257, 3192–3201.
- [10] a) A. Baunemann, D. Rische, A. Milanov, Y. Kim, M. Winter, C. Gemel, R. A. Fischer, *Dalton Trans.* **2005**, 3051–3055; b) A. Baunemann, D. Bekermann, T. B. Thiede, H. Parala, M. Winter, C. Gemel, R. A. Fischer, *Dalton Trans.* **2008**, 3715–3722.
- [11] C. J. Carmalt, A. C. Newport, S. A. O'Neill, I. P. Parkin, A. J. P. White, D. J. Williams, *Inorg. Chem.* **2005**, 44, 615–619.
- [12] a) J. Zhang, R. Cai, L. Weng, X. Zhou, *Organometallics* **2004**, 23, 3303–3308; b) A. P. Kenney, G. P. A. Yap, D. S. Richeson, S. T. Barry, *Inorg. Chem.* **2005**, 44, 2926–2933; c) M. K. T. Tin, G. P. A. Yap, D. S. Richeson, *Inorg. Chem.* **1999**, 38, 998–1001; d) G. Chandra, A. D. Jenkins, M. F. Lappert, R. C. Srivastava, *J. Chem. Soc. A* **1970**, 2550–2558; e) L. L. Anderson, J. A. R. Schmidt, J. Arnold, R. G. Bergman, *Organometallics* **2006**, 25, 3394–3406.
- [13] a) J. Mason, in *Multinuclear NMR*, Plenum Press, New York, **1987**, p. 345; b) J. Mason, L. F. Larkworthy, E. A. Moore, *Chem. Rev.* **2002**, 102, 913–934.
- [14] a) E. P. Beaumier, B. S. Billow, A. K. Singh, S. M. Biros, A. L. Odom, *Chem. Sci.* **2016**, 7, 2532–2536; b) T. J. Hebden, R. R. Schrock, M. K. Takase, P. Muller, *Chem. Commun.* **2012**, 48, 1851–1853; c) R. L. Gdula, M. J. A. Johnson, N. W. Ockwig, *Inorg. Chem.* **2005**, 44, 9140–9142; d) Z. J. Tonzetich, R. R. Schrock, K. M. Wampler, B. C. Bailey, C. C. Cummins, P. Müller, *Inorg. Chem.* **2008**, 47, 1560–1567.
- [15] S. T. Barry, P. G. Gordon, M. J. Ward, M. J. Heikkila, W. H. Monillas, G. P. A. Yap, M. Ritala, M. Leskela, *Dalton Trans.* **2011**, 40, 9425–9430.
- [16] NIST, Gaithersburg, **2012**.
- [17] R. K. Harris, E. D. Becker, S. M. Cabral De Menezes, R. Goodfellow, P. Granger, *Pure Appl. Chem.* **2001**, 73, 1795–1818.
- [18] SHELXTL, Bruker-AXS, Madison, Wisconsin, **2013**.
- [19] SHELXTL2014, Bruker-AXS, Madison, Wisconsin, **2014**.

Received: October 9, 2017